Title	Generation of Nickel Siloxycarbene Complexes from Acylsilanes for the Catalytic Synthesis of Silyl Enol Ethers
Author(s)	Matsuura, Akihisa; Ito, Yuri; Inagaki, Tetsuya et al.
Citation	ACS Catalysis. 2024, 14(23), p. 18216-18222
Version Type	AM
URL	https://hdl.handle.net/11094/100145
rights	This document is the Accepted Manuscript version of a Published Work that appeared in final form in ACS Catalysis, © American Chemical Society after peer review and technical editing by the publisher. To access the final edited and published work see https://doi.org/10.1021/acscatal.4c06272.
Note	

Generation of Nickel Siloxycarbene Complexes from Acylsilanes for the Catalytic Synthesis of Silyl Enol Ethers

Akihisa Matsuura,[a] Yuri Ito,[a] Tetsuya Inagaki,[a] Takuya Kodama[a,b] and Mamoru Tobisu*[a,b]

[a]*Department of Applied Chemistry, Graduate School of Engineering, Osaka University, Suita, Osaka 565-0871, Japan*

[b]*Innovative Catalysis Science Division, Institute for Open and Transdisciplinary Research Initiatives (ICS-OTRI), Osaka University, Suita, Osaka 565-0871, Japan.*

KEYWORDS: nickel catalyst, acylsilane, Fischer carbene complexes, silyl enol ether, DFT calculation

ABSTRACT: A catalytic protocol has been developed to access Fischer carbene nickel complexes using acylsilanes as stable and readily available precursors. The as-generated Fischer carbene complexes exhibit versatile reactivity, including cyclopropanation with alkenes, α-C–H insertion reactions, and two-component C–H addition to norbornene, which demonstrate the broad utility of the nickel(0)/acylsilane system for the catalytic applications of Fischer carbene complexes.

Introduction

Among the transition metal carbene complexes, Fischer carbene complexes, which are characterized by a coordinated carbene carbon bearing electronegative substituents, have held a prominent position in synthetic organic chemistry because of their unique reactivity profiles.[1,2] However, the generation of Fischer carbene complexes normally requires stoichiometric amounts of group 6 metal carbonyl complexes because heteroatom-substituted diazo compounds are unsuitable precursors due to their instability (Scheme 1a). This contrasts with other carbene complexes, which can be generated in situ from the corresponding diazo compounds, facilitating their use in numerous catalytic processes.[3,4] Recently, we reported that Fischer carbene complexes can be generated in situ from acylsilanes via palladium catalysis, enabling catalytic reactions involving Fischer carbene complexes, such as siloxycyclopropanation and β-lactam synthesis (Scheme 1b).[5] Although acylsilanes are known to isomerize to siloxycarbenes under visible-light irradiation or high-temperature conditions (>250 °C),[6] the short lifetime and nucleophilic nature of the resulting metal-free siloxycarbenes limit their applications.[7] Attempts to capture the photochemically generated siloxycarbene with transition metal complexes for the catalytic generation of Fischer carbene complexes have been made; however, this approach has met with limited success, presumably due to the challenge of capturing short-lived metal-free carbene species with a catalytic amount of metal complexes.[8] In this context, our palladium-catalyzed method provides an attractive alternative with potential application to an array of catalytic reactions because it depends solely on organometallic processes and avoids photoirradiation. To further expand the scope of this catalytic method, it is crucial to investigate whether the organometallic process involving the transformation of acylsilanes into siloxycarbene complexes can occur with metal species other than palladium. Herein, we report that nickel complexes can also mediate the generation of a siloxycarbene complex from acylsilanes (Scheme 1c). Importantly, this nickel-mediated organometallic process can be successfully applied not only to catalytic cyclopropanation and α-insertion reactions but also to the unusual catalytic addition to norbornene, which cannot be catalyzed by palladium. It should be noted that photochemical reactions of acylsilanes with external reagents to form silyl enol ethers have also been reported.[9]

Scheme 1. Generation of Siloxycarbene-Metal Complexes from Acylsilanes

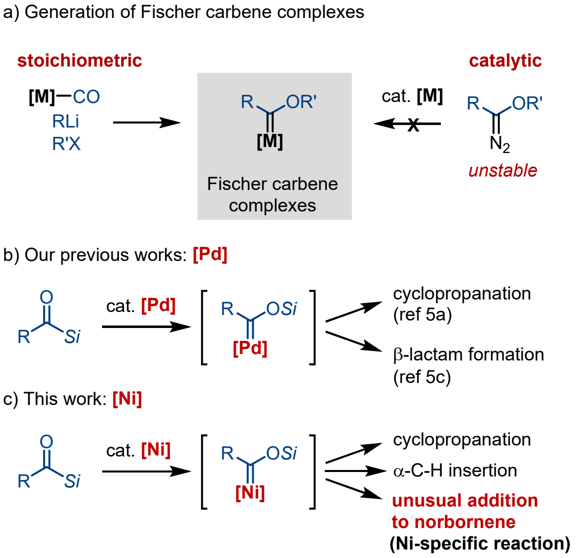

Results and Discussion

We started our investigation by examining a cyclopropanation reaction using acylsilane **1a** and norbornene (**2a**) (Scheme 2). We previously reported that Pd–IPr and Pd–IPr* catalysts can efficiently promote this reaction, with the latter catalyst being more stereoselective (Scheme 2a). When the same reaction was conducted using Ni(cod)$_2$ (20 mol%) as a catalyst and IPr (20 mol%) as a ligand at 160 °C, cyclopropanated product **3a** was obtained in 3% yield (Scheme 2b). Although the major product was decarbonylation product **4a**,[10] the formation of **3a** clearly indicates that nickel can promote the generation of Fischer carbene complexes. When IPr was replaced with the bulkier ligand IPr*, the yield of **3a** increased to 55%. The yield was further improved to 79% by using norbornene as a limiting reagent (i.e., **1a**/**2a** = 2/1). Interestingly, the nickel catalyst afforded considerably better stereoselectivity than the palladium catalyst (24:1 for nickel vs. 6.5:1 for palladium), even though the nickel-catalyzed reactions required harsher conditions.

Scheme 2. Palladium- and Nickel-Catalyzed Cyclopropanation of **2a** with **1a**

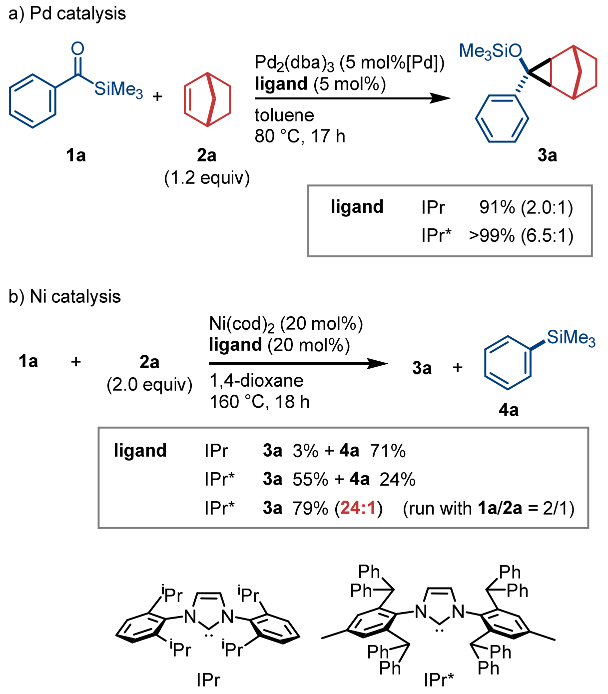

ligand		
	IPr	91% (2.0:1)
	IPr*	>99% (6.5:1)

ligand		
	IPr	**3a** 3% + **4a** 71%
	IPr*	**3a** 55% + **4a** 24%
	IPr*	**3a** 79% (**24:1**) (run with **1a**/**2a** = 2/1)

Next, we compared nickel and palladium catalysts in the reactions of acylsilanes with aliphatic substituents. When acylsilane **1b**, which bears a primary alkyl group, was reacted under the Pd–IPr*-catalyzed conditions, silyl enol ether **5b** was selectively obtained in 78% yield (Scheme 3a). Compound **5b** is presumably formed through an α-C–H insertion reaction of the postulated siloxycarbene complex, which is a common reaction pathway with carbene complexes bearing a β-hydrogen-containing alkyl substituent.[11] In contrast, the nickel-catalyzed reaction of **1b** exclusively yielded decarbonylation product **4b** in 80% yield. Next, acylsilane **1c**, which possesses a cyclohexyl group as a secondary alkyl substituent, was examined (Scheme 3b). In contrast to the reaction of **1b**, **1c** was converted into silyl enol ether **5c** under palladium- and nickel-catalyzed conditions without formation of decarbonylation product **4c**. Interestingly, nickel was a better catalyst than palladium with this specific substrate, as evidenced by the higher yield obtained with nickel (76% yield with nickel vs. 42% yield with palladium). Similarly, acylsilane **1d**, which also contains a secondary alkyl substituent, was also converted into silyl enol ether **5d** in quantitative yield by using a nickel catalyst. Acylsilane **1e** bearing a tertiary alkyl group failed to react irrespective of the catalyst, possibly due to its steric bulk inhibiting the initial oxidative addition of the C(acyl)–Si bond.

Scheme 3. Nickel-catalyzed α-Insertion of Aliphatic Acylsilanes

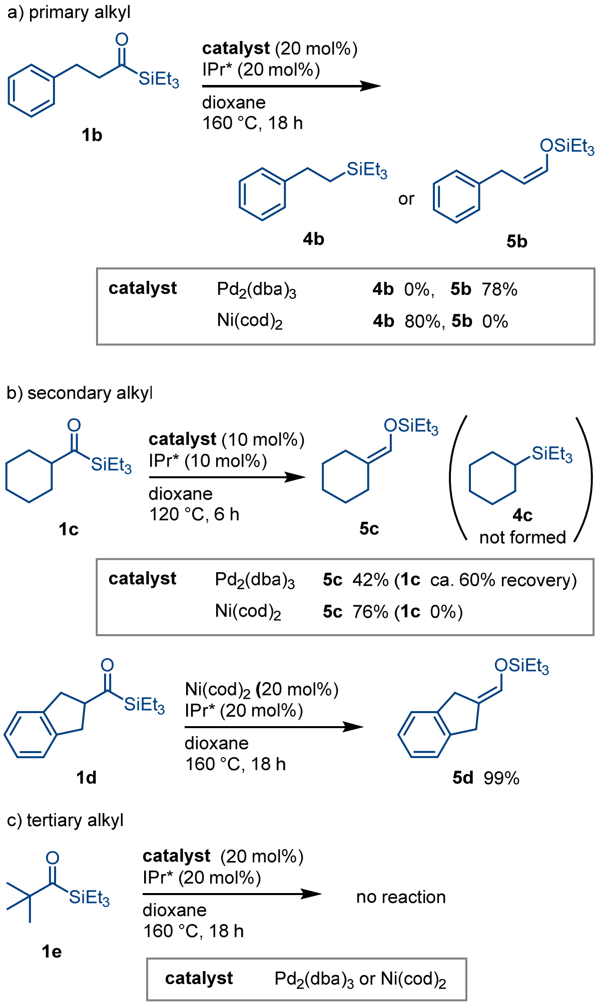

catalyst		
	Pd$_2$(dba)$_3$	**4b** 0%, **5b** 78%
	Ni(cod)$_2$	**4b** 80%, **5b** 0%

catalyst		
	Pd$_2$(dba)$_3$	**5c** 42% (**1c** ca. 60% recovery)
	Ni(cod)$_2$	**5c** 76% (**1c** 0%)

catalyst	
	Pd$_2$(dba)$_3$ or Ni(cod)$_2$

Next, we examined the reactions of aliphatic acylsilanes in the presence of **2a** to examine whether cyclopropanation occurs, as was observed for the reaction of aromatic acylsilane **1a**. The palladium-catalyzed reaction of **1b** with **2a** resulted in the selective formation of silyl enol ether **5b**, without incorporation of **2a** (Scheme 4a). In contrast, using nickel in place of palladium afforded silyl enol ether **6b** (56% isolated yield), in which **2a** was incorporated at the α-position of the siloxy group. It is noteworthy that the decarbonylation pathway was completely suppressed in the presence of **2a** (see Scheme 3a). The palladium and nickel catalysts were also compared in the reaction of secondary alkyl–substituted acylsilane **1c** with **2a** (Scheme 4b). As observed with **1b**, **1c** afforded α-C–H insertion product **5c** using palladium, whereas addition to **2a** occurred to form **6c** in the case of nickel. The structure of **6c** was unambiguously determined by means of an X-ray crystallography analysis of the derivatized hydrazone **7c** (Scheme 4c). The nickel-catalyzed reaction of aliphatic acylsilanes with **2a** was found to be general, as evidenced by the formation of **6d** and **6f** from acylsilanes **1d** and **1f**, respectively. Meanwhile, using other alkenes instead of **2a**, such as 1-octene, styrene, vinyltrimethylsilane, *tert*-butyl acrylate, and acenaphthylene, did not afford the corresponding products under these nickel-catalyzed conditions.

Scheme 4. Nickel-Catalyzed Synthesis of Silyl Enol Ethers from Alkanoylsilanes and **2a**

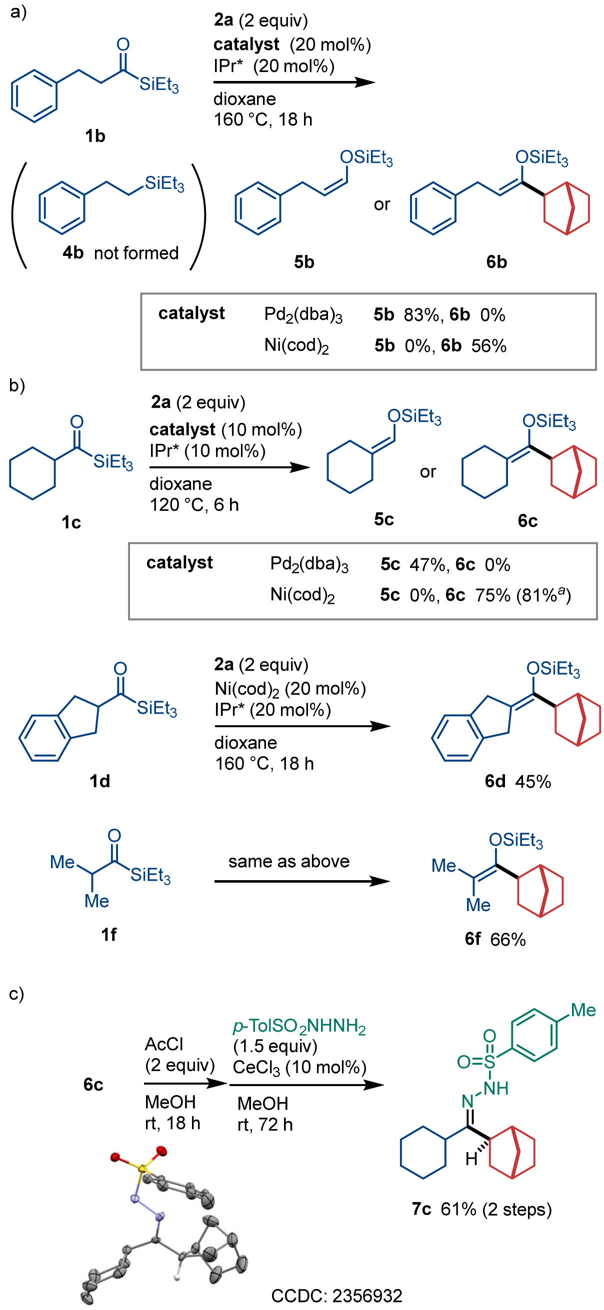

[a]Run with **2a** (3 equiv), Ni(cod)$_2$ (20 mol%), and IPr* (20 mol%) at 160 °C for 18 h.

We conducted several mechanistic studies to obtain insights into the reaction mechanism. When silyl enol ether **5c** was reacted with **2a** under the standard nickel-catalyzed conditions, no reaction occurred (Scheme 5a), which allowed excluding **5c** as an intermediate for the formation of **6c**. Next, the reaction with labeled substrate **1c-*d***, in which the α-position of the acylsilane was deuterated (Scheme 5b), furnished silyl enol ether **6c-*d*** with the 98% of the deuterium being incorporated into the 3-position of the norbornane skeleton in a stereoselective manner.

Scheme 5. Mechanistic Studies

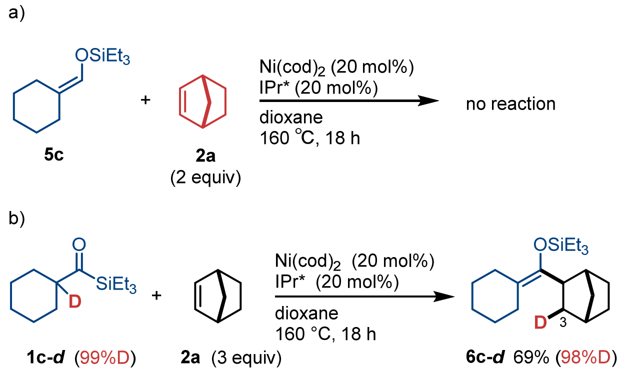

We investigated computationally the origin of the different behaviors between palladium and nickel using density functional theory (DFT) calculations at the ωB97XD/SDD-6-311+G(d,p)-SDD//ωB97XD/LANL2DZ-6-31G(d,p)-SDD level of theory (Scheme 6). First, we examined the palladium-catalyzed reactions of primary alkyl–substituted acylsilane (Scheme 6a). The initial oxidative addition of the C(acyl)–Si bond was found to proceed with an activation barrier of 8.6 kcal/mol to form **INT1** (see SI for details). The oxidative addition complex **INT1** can then undergo two possible pathways. One is the extrusion of CO to form **INT2**; however, this is an unfavorable endothermic process (ΔG = +21.1 kcal/mol) with a high activation barrier of 26.2 kcal/mol. In contrast, 1,3-migration of a silyl group in **INT1** to form siloxycarbene complex **INT3** would occur in an exothermic manner (ΔG = −1.0 kcal/mol) with a lower activation barrier (22.3 kcal/mol), which renders this pathway more favored than decarbonylation. Subsequently, **INT3** undergoes insertion into an α-C–H bond via **TS3** to form **INT4**. Similarly, in the case of a secondary alkyl–substituted substrate, the activation barrier for decarbonylation from the corresponding oxidative addition complex **INT5**[12] was substantially higher than that required for the α-insertion reaction.[13] These results are in agreement with the experimental observation that alkyl-substituted acylsilanes led exclusively to α-insertion products rather than decarbonylation products (Scheme 3a, b).

Scheme 6. Plausible Reaction Pathways for the Palladium-Catalyzed System[a]

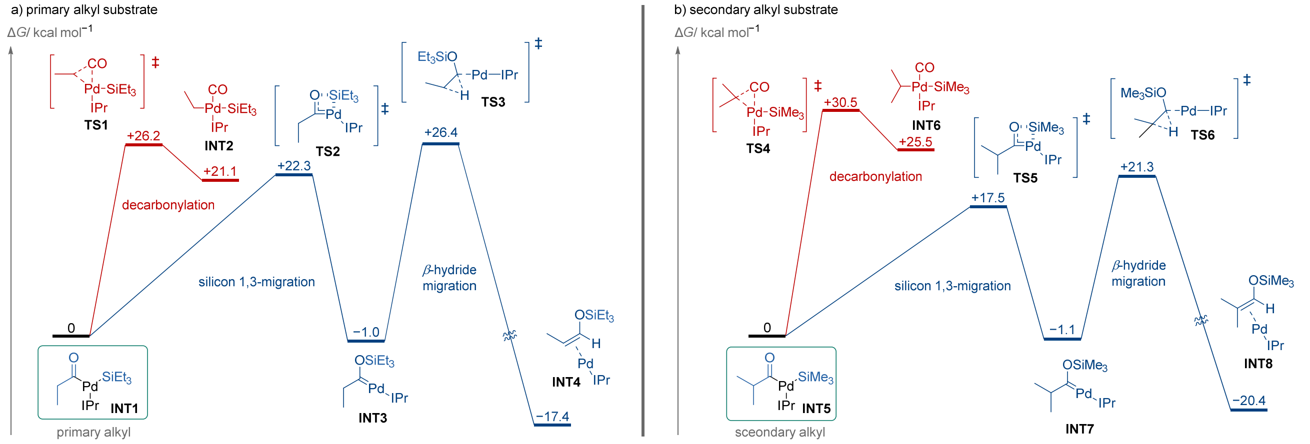

[a] DFT calculations were conducted at the ωB97XD/6-311+G(d,p)-SDD//ωB97XD/6-31G(d,p)-Lanl2DZ level of theory. Red: decarbonylation; blue: α-insertion via a siloxycarbene-palladium complex.

A similar comparison was also performed for the nickel-catalyzed system (Scheme 7). In the case of primary alkyl–substituted acylsilanes, the activation barrier for decarbonylation from oxidative addition complex **INT9**[14] was considerably lower (9.8 kcal/mol, **TS7**) than that required with the Pd catalyst (26.2 kcal/mol, **TS1** in Scheme 6).[15] Meanwhile, the activation barriers for the formation of the silyl enol ether via siloxycarbene-nickel complex **INT11** were comparable to those calculated for the palladium catalyst (19.0 kcal/mol for **TS8** and 25.1 kcal/mol for **TS9**). These results are consistent with the experimental observation that decarbonylation occurred with the nickel catalyst when primary alkyl–substituted acylsilanes were used (Scheme 3a). In the case of secondary alkyl–substituted substrates, the activation barrier required for decarbonylation from oxidative addition complex **INT14**[16] increased to 22.0 kcal/mol (i.e., **TS11**), possibly due to the increased steric demand for C–C bond activation, which makes the α-C–H insertion pathway more energetically feasible, as was experimentally observed (Scheme 3b). It should be noted that the mechanism for the α-insertion from siloxycarbene-nickel complexes (*i.e.*, **INT11** or **INT16**) differs from that involving the palladium catalyst. While siloxycarbene-palladium complexes undergo α-C–H insertion in a concerted manner without any intermediate (Scheme 6), a β-hydrogen elimination/reductive elimination sequence occurs in the case of siloxycarbene-nickel complexes via a nickel-hydride intermediate (i.e., **INT12** or **INT17**) to form α-insertion products.

Scheme 7. Plausible Reaction Pathways for the Nickel-Catalyzed System[a]

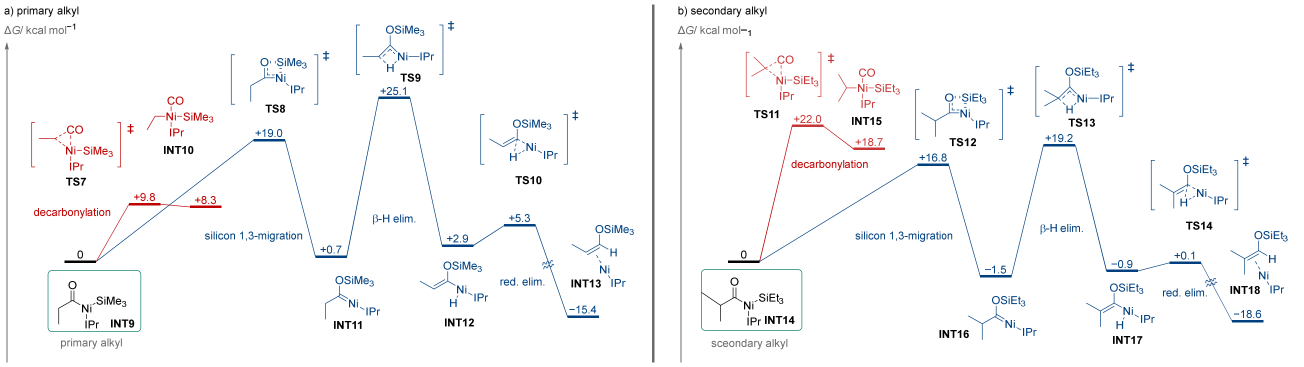

[a]DFT calculations were conducted at the ωB97XD/6-311+G(d,p)-SDD//ωB97XD/6-31G(d,p)-Lanl2DZ level of theory. Red: decarbonylation; blue: α-insertion via a siloxycarbene-nickel complex.

Finally, we investigated the mechanism for the nickel-catalyzed reaction of aliphatic acylsilanes with norbornene via DFT calculations using the reaction of isopropyl-substituted acylsilane with ethylene catalyzed by a Ni–IPr complex as a model reaction (Scheme 8). The oxidative addition of the C(acyl)–Si bond to the Ni–IPr complex was revealed to proceed via three-centered transition state **TS15** with an activation barrier of 18.2 kcal/mol, leading to the formation of oxidative addition complex **INT20**. Intermediate **INT20** can isomerize through migration of the silyl group to the oxygen atom of the acyl ligand via **TS16** with a feasible energetic barrier (20.4 kcal/mol), furnishing siloxycarbene-nickel complex **INT21**. Upon addition of ethylene, **INT21** forms a more stable three-coordinate complex, i.e., **INT22**, which subsequently undergoes a concerted α-C–H insertion through transition state **TS15** to produce silyl enol ether–ligated nickel complex **INT23**. This α-C–H insertion process, which requires the highest activation barrier (30.3 kcal/mol) during the reaction pathway, is the turnover-limiting step. Subsequently, **INT23** undergoes ligand-to-ligand hydrogen transfer (LLHT)[17] via **TS18** (3.4 kcal/mol) to form **INT24**. The resulting intermediate **INT24** affords the silyl enol ether product via reductive elimination.

Scheme 8. DFT-Computed Energy Profile for the Nickel-Catalyzed Reaction of Aliphatic Acylsilanes with Ethylene to Form Silyl Enol Ethers

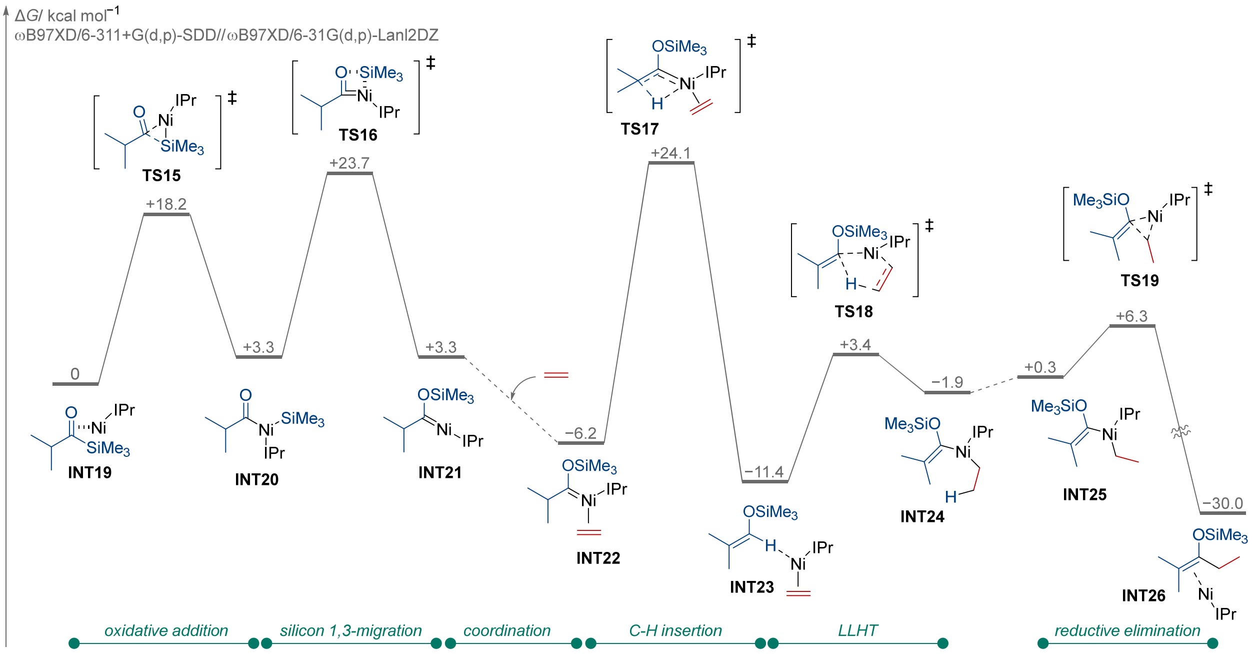

According to the experimental and theoretical studies discussed above, a plausible mechanism for the nickel-catalyzed reactions of aliphatic acylsilanes is depicted in Scheme 9. First, the C(acyl)–Si bond of the acylsilane substrate is oxidatively added to the nickel catalyst to form **A**, which can then undergo two possible pathways. When a primary alkyl–substituted acylsilane is used in the absence of **2a**, complex **A** predominantly undergoes decarbonylation. This decarbonylation pathway can be suppressed by adding **2a**, presumably because it occupies a vacant coordination site that is required for the decarbonylation, or by using bulkier secondary alkyl–substituted acylsilane substrates. In these cases, the silicon group in **A** migrates to the oxygen atom to form siloxycarbene-nickel complex **B**. Carbene complex **B** undergoes α-C–H insertion via nickel-hydride **C** to furnish a silyl enol ether when secondary alkyl–substituted acylsilanes are reacted in the absence of **2a**. Meanwhile, in the presence of **2a**, carbene complex **B** undergoes α-C–H insertion in a concerted manner to form enol ether complex **E**,[18] which immediately forms alkenyl-nickel species **F** via LLHT. Subsequent reductive elimination from **F** affords two-component coupling product **G**.

Scheme 9. Plausible Mechanism for the Nickel-Catalyzed Reactions of Aliphatic Acylsilanes

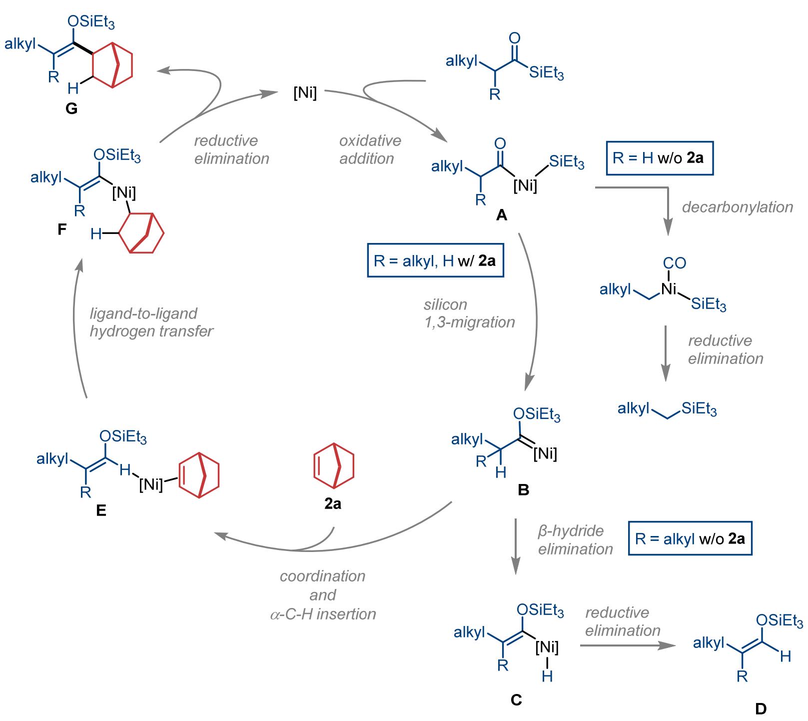

Conclusion

In summary, we have demonstrated that generation of siloxycarbene complexes from acylsilanes via oxidative addition of a C–Si bond followed by 1,3-silicon migration is not limited to palladium but can be also catalyzed by nickel. This protocol enables the generation of otherwise inaccessible Fischer carbene complexes of nickel. When aromatic acylsilanes are used, the resulting siloxycarbene-nickel intermediate undergoes cyclopropanation with alkenes, as in the case of palladium. Nickel-catalyzed reactions of aliphatic acylsilanes follow two distinct pathways depending on the bulkiness of the acyl substituents: primary alkyl–substituted acylsilanes afford decarbonylation products, whereas substrates with secondary alkyl groups form silyl enol ethers via α-C–H insertion from a siloxycarbene-nickel intermediate. These results contrast sharply with those obtained using the palladium-catalyzed system, which uniformly provides silyl enol ethers from aliphatic acylsilanes. Most notably, nickel-catalyzed reactions of aliphatic acylsilanes with norbornene furnish two-component coupling products, in which a C–H bond of the silyl enol ethers adds across norbornene. These findings underscore that the reactivity of siloxycarbene complexes is markedly influenced by the nature of the metal center, enabling new catalytic transformations using acylsilanes. Studies on further applications of siloxycarbene-Pd and -Ni complexes, as well as exploration of other late transition metals, are currently underway in our laboratory.

Methods

Typical Procedure for Nickel-Catalyzed Synthesis of Silyl Enol Ethers from Alkanoylsilanes with Norbornene.

In a glove box, to an oven-dried 10 mL screw-capped vial, Ni(cod)$_2$ (11.0 mg, 0.040 mmol), IPr* (36.6 mg, 0.040 mmol), acylsilane **1b** (49.7 mg, 0.20 mmol), **2** (38.8 mg, 0.40 mmol), and 1,4-dioxane (1.0 mL) were added. The cap was closed and the resulting mixture was stirred at 160 °C for 18 h. After cooling to rt, the resulting mixture was filtered through a celite pad. The filtrate was concentrated to dryness in vacuo and the residue was purified by silica gel column chromatography (hexane to hexane/EtOAc = 1/9) to afford the desired product **6b** as a colorless oil (38.2 mg, 56% yield).

ASSOCIATED CONTENT

Supporting Information

The Supporting Information is available free of charge on the ACS Publications website.

Detailed experimental procedures, characterization of new compounds and computational details (PDF)

Compound **7c** crystal structure (CIF)

AUTHOR INFORMATION

Corresponding Author

*tobisu@chem.eng.osaka-u.ac.jp

Notes

The authors declare no competing financial interests.

ACKNOWLEDGMENT

This work was supported by KAKENHI (JP21H04682, JP24H02206 and JP24H02207) from MEXT, Japan. A.M. thanks a JSPS Research Fellowship for Young Scientists (23KJ1433) for financial support. T.I. thanks a JSPS Research Fellowship for Young Scientists (23KJ1498) for financial support. Theoretical calculations were partly performed using the Research Center for Computational Science, Okazaki, Japan (Project: 23-IMS-C304, 24-IMS-C113). We also thank the Instrumental Analysis Center, Graduate School of Engineering, Osaka University, for their assistance with HRMS.

REFERENCES

(1) Fischer, E. O.; Maasböl, A. On the Existence of a Tungsten Carbonyl Carbene Complex. *Angew. Chem. Int. Ed.* **1964**, *3*, 580–581.

(2) (a) Dötz, K. H. Carbene Complexes in Organic Synthesis [New Synthetic Methods]. *Angew. Chem. Int. Ed.* **1984**, *23*, 587–608. (b) de Meijere, A.; Schirmer, H.; Duetsch, M. Fischer Carbene Complexes as Chemical Multitalents: The Incredible Range of Products from Carbenepentacarbonylmetal α,β-Unsaturated Complexes. *Angew. Chem. Int. Ed.* **2000**, *39*, 3964–4002. (c) Gómez-Gallego, M.; Mancheño, M. J.; Sierra, M. A. Catalytic Transmetalation from Group 6 Fischer Carbene Complexes: An Emerging Powerful Tool in Organic Synthesis. *Acc. Chem. Res.* **2005**, *38*, 44–53. (d) Dötz, K. H.; Stendel, J. Jr. Fischer Carbene Complexes in Organic Synthesis: Metal-Assisted and Metal-Templated Reactions. *Chem. Rev.* **2009**, *109*, 3227–3274. (e) Raubenheimer, H. G. Fischer Carbene Complexes Remain Favourite Targets, and Vehicles for New Discoveries. *Dalton Trans.* **2014**, *43*, 16959–16973. (f) Feliciano, A.; Vázquez, J. L.; Benítez-Puebla, L. J.; Velazco-Cabral, I.; Cruz Cruz, D.; Delgado, F.; Vázquez, M. A. Fischer Carbene Complexes: A Glance at Two Decades of Research on Higher-Order Cycloaddition Reactions. *Chem. Eur. J.* **2021**, *27*, 8233–8251. (g) Zhou, G.; Guo, Z.; Shen, X. Electron-Rich Oxycarbenes: New Synthetic and Catalytic Applications beyond Group 6 Fischer Carbene Complexes. *Angew. Chem. Int. Ed.* **2023**, *62*, e202217189.

(3) He, Y.; Huang, Z.; Wu, K.; Ma, J.; Zhou, Y.-G.; Yu, Z. Recent Advances in Transition-Metal-Catalyzed Carbene Insertion to C–H Bonds. *Chem. Soc. Rev.* **2022**, *51*, 2759–2852.

(4) While N-heterocyclic carbene and related complexes have been reported, these carbene ligands typically serve as supporting ligands and do not exhibit reactivity typical of Fischer carbenes, such as cyclopropanation or C-H insertion. For example, see: Kremzow, D.; Seidel, G.; Lehmann, C. W.; Fürstner, A., Diaminocarbene- and Fischer-Carbene Complexes of Palladium and Nickel by Oxidative Insertion: Preparation, Structure, and Catalytic Activity. *Chem.–Eur. J.* **2005**, *11*, 1833-1853.

(5) (a) Sakurai, S.; Inagaki, T.; Kodama, T.; Yamanaka, M.; Tobisu, M. Palladium-Catalyzed Siloxycyclopropanation of Alkenes Using Acylsilanes. *J. Am. Chem. Soc.* **2022**, *144*, 1099–1105. (b) Sakurai, S.; Inagaki, T.; Kodama, T.; Yamanaka, M.; Tobisu, M. Pd-Catalyzed Siloxycyclopropanation of Alkenes. *Trends in Chemistry* **2022**, *4*, 1161–1162. (c) Inagaki, T.; Kodama, T.; Tobisu, M. Catalytic Synthesis of β-Lactam Derivatives by Carbonylative Cycloaddition of Acylsilanes with Imines via a Palladium Fischer-Carbene Intermediate. *Nat. Catal.* **2024**, 1–7. (d) Inagaki, T.; Akita, Y.; Tobisu, M. Palladium-Catalyzed Addition of Trifluoroacetylsilanes to Alkenes and Allenes via the Cleavage of C–Si Bonds. *Org. Lett.* **2024**, *26*, 2141–2145.

(6) Brook, A. G. Triphenylsilyl Phenyl Ketone. *J. Am. Chem. Soc.* **1957**, *79*, 4373–4375.

(7) (a)Zhao, Q.; Geng, Q.; Li, Y.; Li, J.; Liu, Z. Emerging Applications of Acylsilanes in Organic Synthesis and Beyond. *Org. Chem. Front.* **2023**. (b) Hong, W. P.; Lim, H. N.; Shin, I. Recent Progress and Perspectives in Photo-Induced Organic Reactions of Acylsilanes. *Org. Chem. Front.* **2023**, *10*, 819–836. (c) Guo, Y.; Zhou, G.; Shen, X. Synthesis of Organofluorine Compounds with Acylsilanes†. *Chin. J. Chem.* **2024**, *42*, 887–902.

(8) (a) Takeuchi, T.; Aoyama, T.; Orihara, K.; Ishida, K.; Kusama, H. Visible-Light-Induced In Situ Generation of Fischer-Type Copper Carbene Complexes from Acylsilanes and Its Application to Catalytic [4 + 1] Cycloaddition with Siloxydienes. *Org. Lett.* **2021**, *23*, 9490–9494. (b) Ueda, Y.; Masuda, Y.; Iwai, T.; Imaeda, K.; Takeuchi, H.; Ueno, K.; Gao, M.; Hasegawa, J.; Sawamura, M. Photoinduced Copper-Catalyzed Asymmetric Acylation of Allylic Phosphates with Acylsilanes. *J. Am. Chem. Soc.* **2022**, *144*, 2218–2224. (c) Zheng, L.; Guo, X.; Li, Y.-C.; Wu, Y.; Xue, X.-S.; Wang, P. Cu/SaBox-Catalyzed Photoinduced Coupling of Acylsilanes with Alkynes. *Angew. Chem. Int. Ed.* **2022**, anie.202216373. (d) Zheng, L.; Li, Y.-C.; Wu, Y.; Wang, P. Photoinduced Copper-Catalyzed Cross-Coupling of Acylsilanes with Azoles. *ChemRxiv* January 2, 2024: 10.26434/chemrxiv-2024-6x3q7.

(9) (a) Fang, X.; Wen, S.; Jin, P.; Bao, W.; Liu, S.; Cong, H.; Shen, X. Synthesis of Enantioenriched Fluorinated Enol Silanes Enabled by Asymmetric Reductive Coupling of Fluoroalkylacylsilanes and 1,3-Enynes and Brook Rearrangement. *ACS Catal.* **2022**, *12*, 2150–2157. (b) Zhou, G.; Guo, Z.; Liu, S.; Shen, X. Divergent Synthesis of Fluoroalkyl Ketones through Controlling the Reactivity of Organoboronate Complexes. *J. Am. Chem. Soc.* **2024**, *146*, 4026–4035. (c) Liu, Y.; Zhu, Z.; Zhang, Y.; Zhang, Y.; Liu, S.; Shen, X. Stereoselective Synthesis of Silyl Enol Ethers with Acylsilanes and α,β-Unsaturated Ketones. *Org. Lett.* **2024**, *26*, 5911–5916.

(10) Nakatani, S.; Ito, Y.; Sakurai, S.; Kodama, T.; Tobisu, M. Nickel-Catalyzed Decarbonylation of Acylsilanes. *J. Org. Chem.* **2020**, *85*, 7588–7594.

(11) (a) Taber, D. F.; Hennessy, M. J.; Louey, J. P. Rhodium-Mediated Cyclopentane Construction Can Compete with β-Hydride Elimination: Synthesis of (±)-Tochuinyl Acetate. *J. Org. Chem.* **1992**, *57*, 436–441. (b) Taber, D. F.; Hoerrner, R. S. Enantioselective Rhodium-Mediated Synthesis of (−)-PGE2 Methyl Ester. *J. Org. Chem.* **1992**, *57*, 441–447. (c) Muthusamy, S.; Gunanathan, C.; Babu, S. A. Rhodium(II) Acetate Catalyzed Synthesis of Cyclic Enamides and Enamines via β-Hydride Elimination. *Synthesis* **2002**, *2002*, 471–474. (d) Solé, D.; Amenta, A.; Mariani, F.; Bennasar, M.-L.; Fernández, I. Transition Metal-Catalysed Intramolecular Carbenoid C–H Insertion for Pyrrolidine Formation by Decomposition of α-Diazoesters. *Adv. Synth. Catal.* **2017**, *359*, 3654–3664. (e) Polukeev, A. V.; Wendt, O. F. Cyclohexane-Based Phosphinite Iridium Pincer Complexes: Synthesis, Characterization, Carbene Formation, and Catalytic Activity in Dehydrogenation Reactions. *Organometallics* **2017**, *36*, 639–649.

(12) The activation barrier for the oxidative addition of isopropyl-substituted acylsilane catalyzed by Pd–IPr to form **INT5** was +8.4 kcal/mol. See SI for details.

(13) DeAngelis, A.; Dmitrenko, O.; Fox, J. M. Rh-Catalyzed Intermolecular Reactions of Cyclic α-Diazocarbonyl Compounds with Selectivity over Tertiary C–H Bond Migration. *J. Am. Chem. Soc.* **2012**, *134*, 11035–11043.

(14) The activation barrier for the oxidative addition of ethyl-substituted acylsilane catalyzed by Ni-IPr to form **INT9** was +18.4 kcal/mol. See SI for details.

(15) A similar behavior was also observed in the catalytic decarbonylative cross-coupling of phenyl esters, in which nickel exhibits superior activity than palladium: (a) Amaike, K.; Muto, K.; Yamaguchi, J.; Itami, K. Decarbonylative C–H Coupling of Azoles and Aryl Esters: Unprecedented Nickel Catalysis and Application to the Synthesis of Muscoride A. *J. Am. Chem. Soc.* **2012**, *134*, 13573–13576. (b) Ben Halima, T.; Zhang, W.; Yalaoui, I.; Hong, X.; Yang, Y.-F.; Houk, K. N.; Newman, S. G. Palladium-Catalyzed Suzuki–Miyaura Coupling of Aryl Esters. *J. Am. Chem. Soc.* **2017**, *139*, 1311–1318. (c) Liu, C.; Li, G.; Shi, S.; Meng, G.; Lalancette, R.; Szostak, R.; Szostak, M. Acyl and Decarbonylative Suzuki Coupling of N-Acetyl Amides: Electronic Tuning of Twisted, Acyclic Amides in Catalytic Carbon–Nitrogen Bond Cleavage. *ACS Catal.* **2018**, *8*, 9131–9139. (d) Li, R.; Xu, H.; Zhao, N.; Jin, X.; Dang, Y. Origins of Chemoselectivity in the Ni-Catalyzed Biaryl and Pd-Catalyzed Acyl Suzuki–Miyaura Cross-Coupling of N-Acetyl-Amides. *J. Org. Chem.* **2020**, *85*, 833–840. (e) Liu, J.; Ling, M.; Xie, H. Mechanisms of Chemoselectivity for Acyl and Decarbonylative Suzuki–Miyaura Coupling of *N*-Acetyl Amide with Arylboronic Acid Catalyzed by Pd and Ni Catalysts: Insights from DFT Calculations. *Comput. Theor. Chem.* **2020**, *1185*, 112889.

(16) The activation barrier for the oxidative addition of acylsilane by Ni–IPr to form **INT14** was +17.5 kcal/mol. See SI for details.

(17) Guihaumé, J.; Halbert, S.; Eisenstein, O.; Perutz, R. N. Hydrofluoroarylation of Alkynes with Ni Catalysts. C–H Activation via Ligand-to-Ligand Hydrogen Transfer, an Alternative to Oxidative Addition. *Organometallics* **2012**, *31*, 1300–1314.

(18) The reaction did not proceed when using silyl enol ether as a starting material (Scheme 5a) most likely due to the relative instability of complex **E** compared with Ni(cod)IPr, which makes the ligand exchange process unfavorable. Calculations revealed that the ligand exchange of the Ni(norbornene)$_2$IPr complex to the corresponding enol ether–bound complex similar to **E** is endergonic by 73.3 kcal/mol. See SI for details.